



Visualizing Samsonfish (*Seriola hippos*) with a Reson 7125 Seabat multibeam sonar

Miles J. G. Parsons*, Iain M. Parnum, and Robert D. McCauley

Centre for Marine Science and Technology, Curtin University, GPO Box U1987, Perth, WA 6845, Australia

*Corresponding Author: tel: +61 8 9266 7380; fax: +61 8 9266 4799; e-mail: m.parsons@cmst.curtin.edu.au

Parsons, M. J. G., Parnum, I. M., and McCauley, R. D. 2013. Visualizing Samsonfish (*Seriola hippos*) with a Reson 7125 Seabat multibeam sonar – ICES Journal of Marine Science, 70: 665–674.

Received 20 August 2012; accepted 15 January 2013; advance access publication 24 February 2013.

In Western Australia, aggregations of Samsonfish (*Seriola hippos*) form each summer to spawn in waters west of Rottnest Island. In this study, a Reson 7125 Seabat multibeam sonar (400 kHz) was pole mounted aboard a 21.6 m vessel, conducting acoustic transects to acquire acoustic backscatter simultaneously from a midwater aggregation of *S. hippos* and the wreck it surrounded. The processed backscatter produced high-resolution visualizations of both the fish and seabed. During a 15 min period, the centroid of the aggregation moved 91 m around the eastern and northeastern side of the wreck and probably exhibited lateral vessel avoidance behaviour from the survey vessel. Additionally, a northeasterly current at the site was inferred from subtle habitat features, suggesting that at the time of the survey the aggregation preferred to remain upcurrent of the wreck. These findings confirmed that the *S. hippos* aggregations do not necessarily remain directly above the wrecks and do not always remain sedentary. Aggregation acoustic density packing at the survey site was observed at $12.7 \pm 2.4 \text{ m}^3$ per fish, equivalent to $\sim 1.6 \pm 0.1$ body lengths nearest-neighbour distance.

Keywords: backscatter, fisheries, habitat classification, multibeam.

Introduction

Concerns over climatic and anthropogenic impacts, combined with increasing fishing pressures on fish stocks, have made the evolution from single species management to ecosystem-based fishery management (EBFM) an intrinsic component in maintaining sustainable fisheries worldwide (Pikitch *et al.*, 2004). Therefore, rapid, accurate, and replicable quantification of classified fish schools and identification of their associated essential fish habitats have become significant objectives of EBFM and fishery acoustics.

Over the past two decades, multibeam sonar (MBS) systems, traditionally designed to acquire bathymetric data, evolved to provide information on habitat types from their acoustic reflectance (Brown and Blondel, 2009; Brown *et al.*, 2011; Parnum and Gavrilov, 2011a, b). Backscatter from faunal targets in the water column has been increasingly investigated (Mayer *et al.*, 2002; Trenkel *et al.*, 2006; Ona *et al.*, 2006; Holmin *et al.*, 2009; Korneliussen *et al.*, 2009; Patel and Ona, 2009; Stienessen *et al.*, 2009), sometimes combined with single- or split-beam systems (Weber *et al.*, 2007; Korneliussen *et al.*, 2009) or with adapted mounting positions for shallow waters (Gerlotto *et al.*, 1998). Several fishery-designed sonar systems have been developed with water column sampling in mind, including the Simrad SM2000

and MS 70, sometimes with the option to collect bathymetric data (Simrad ME 70 www.simrad.com; Andersen *et al.*, 2006; Trenkel *et al.*, 2008). However, the ability to acquire and store adequately sampled water column data in addition to seabed backscatter data can inhibit the ping rate and hence the along-track resolution of several MBS systems (Trevorrow, 2005; Parsons, 2010).

The Reson 8125 MBS was traditionally used for hydrographic purposes. Parsons *et al.* (2006) used a Reson 8125 to investigate Samsonfish (*Seriola hippos*) aggregations, and illustrated that while the sample resolution of an individual Reson 8125 swathe was sufficient to identify individual *S. hippos* targets and collect significant backscatter data from the seabed, there were limitations in alongship resolution due to the ping rate. Such findings were in agreement with previous MBS studies (also using a Reson 8125) investigating fish at similar depths (Trevorrow, 2005). For accurate quantification of fish numbers and behaviour, it is essential that the ping rate is sufficient to remove spatial aliasing. Subsequent to the survey in this study, an adaptation to a more recent system, the Reson 7125, means it is now capable of sampling water column and seabed acoustic backscatter at a resolution of 4 cm and 40 pings s^{-1} , greatly improving alongship resolution.

While currently of limited commercial importance in Australia, *S. hippos* is a physically strong pelagic species and forms a large sport fishery (Rowland, 2009). A spawning aggregation is defined by Domeier and Colin (1997) as, “a group of con-specific fish gathered for the purpose of spawning with fish densities or numbers significantly higher than those found in the area of aggregation during non-reproductive periods”. Each year, thousands *S. hippos* migrate along the Western Australian coastline to form such aggregations in waters off the Perth coast. Similar to other species of fish, *S. hippos* use the habitat provided by submerged structures [fish aggregating devices (FADs), seamounts, wrecks, etc.] as a meeting point to aggregate (Castro *et al.*, 2002; Rowland, 2009; Karnauskus *et al.*, 2011). Approximately 6 nautical miles west of Rottneest Island, a number of man-made wrecks lie in sandy seabed in ~ 100 m of water (Figure 1). The aggregations that form here remain for several months, between October and March. Charter fishing boat operators consider these aggregations to be predominantly sedentary, excellent for novice and experienced sport fishers alike (Rowland, 2009). The inter- and intraseasonal patterns of the formation and duration of the aggregations have been identified in general, and variations in aggregation size, choice of wreck, and duration have been observed, but what environmental or biological factors drive these changes is unknown (Parsons, 2010). While the broad-scale mapping of these wrecks and the habitat they offer the aggregations is known, subtle variations which may affect the dynamics of the aggregations have not been identified. The species possess a large swimbladder, an effective acoustic reflector (Rowland, 2009; Parsons, 2010). Together with the size of the aggregations, apparent lack of mobility, and predictable, prolonged formation combined with the strong acoustic reflectance by the *S. hippos* swimbladder makes the species and location an excellent case study for applying the techniques of an MBS acoustic survey.

The purpose of this research was to acquire backscatter simultaneously from the midwater targets and their surrounding habitat. This was to test the resolution at which the Reson 7125 could acquire both types of data, and to determine whether the *S. hippos* aggregations are at times mobile and the level at which MBS is capable of observing any movement.

Methods

Operating at 400 kHz, the Reson 7125 generates a transmit beam nominally of width 1° alongship and 155° athwartship. An orthogonal line array forms an effective beam pattern of 512 equidistant beams across a $128^\circ \times 1^\circ$ swathe of up to 456 samples per metre at a maximum resolution of 2.5 cm (Reson Incorporated, 2006). The sonar acquires data at a rate of ~ 155 Gbyte h^{-1} (at a range of 100 m with a 5 Hz ping rate), thus requiring 2 Tbyte of storage per survey day (Malzone *et al.*, 2008). Recent advances in post-processing techniques allow mining of considerable data volumes from entire surveys to provide the observation of detected schools in time and space (Wilson *et al.*, 2005; Buelens *et al.*, 2007). One such Reson 7125 was mounted aboard the RV *Naturaliste*, a 21.6 m fishery vessel, to investigate an aggregation of *S. hippos*. The sonar head was positioned 3.95 m from the vessel centreline and 2.77 m below the water surface. Nadir beams were directed vertically downwards.

Calibration techniques (Chu *et al.*, 2002; Foote *et al.*, 2005) were not applied to the Reson 7125. The lack of system calibration eliminates the possibility of abundance estimates using echo-integration techniques to estimate abundance and length distribution. However, given the relatively small number of fish, the

limited time available for the survey, and the number of variables to consider (three-dimensional reflectance pattern of the fish, unknown orientation of the fish), accurate abundance estimates would be unlikely. Moreover, the size of *S. hippos* suggests that individual target counting would be a more feasible method of estimating abundance.

The *S. hippos* are known to migrate from as far around the southwest coast of Australia as Hopetoun (Figure 1) where they spend the winter months, feeding to build up body mass for the spawning period (Rowland, 2009). There are numerous spawning sites around Perth; however, this study reports on acoustic backscatter acquired from a site known as the “Outer Patch”, a prominent site (Parsons, 2010). This is an area ~ 6 nautical miles west of Rottneest Island (Figure 1), containing a wreck, lying partially buried 110 m deep on a flat, sandy seabed. This site annually hosts an acoustically detectable aggregation of *S. hippos* (Parsons *et al.*, 2005; Parsons, 2010). Acoustic transects of ~ 500 m in length were conducted running north–south and south–north along the length of the wreck during the mornings of 2 and 3 February 2007, each transect lasting a maximum of 3 min.

Preliminary transects were conducted at the Outer Patch (as well as at other sites) on 2 February to estimate optimal settings of power, gain, and pulse length for acquiring sufficient backscatter responses from the aggregation and seabed. These settings were to ensure responses from individual fish were detected while the response from a dense group of fish was not saturated. Individual beam responses from densely populated areas of the aggregation were monitored visually using Reson 7125 software to ensure received backscatter remained unsaturated. As these transects utilized a number of different settings and speeds, their results have not been shown here. Optimum settings were determined as a pulse rate of 150 μs , power of 220 dB, gain of 25 dB, and range of 175 m, with the maximum available ping rate of one ping every 1.2 s at this range. The combined vessel speed and ping rate resulted in ~ 2.3 – 2.9 m between each acoustic swathe (excluding effects of pitch and yaw). At the typical *S. hippos* aggregation depths of between ~ 60 and 90 m, the widths of the swathe in the alongship direction were 1.05 and 1.57 m, respectively. Interping distance and acoustic beam widths resulted in approximate ranges of 1.25–1.85 m at 60 m and 0.73–1.33 m at 90 m between consecutive acoustic swathes (excluding pitch and yaw). At 90 m, the Reson 7125 swathe was theoretically > 350 m wide, capable of encompassing the width of the entire aggregation. Roll data were imported into each file, including an initial system tilt angle of 3.9° to port. A Kalman filter was applied to smooth GPS and heading data in order to limit the effects of yaw on overlapping pings.

During transects, the vessel speed was maintained, as consistently as possible, between 4 and 5 knots, in ~ 10 knot winds and 1 m seas. Ships position was recorded each second using a Furuno Differential GPS system. Octopus F180 and Applanix POSMV motion sensors supplied pitch, roll, and yaw data, which were logged in real time together with the sound velocity profile using PDS2000 software. Towed underwater video transects were conducted before and after acoustic surveys to verify species presence and confirm aggregation structure.

Side-lobe noise and electrical noise were removed from the data using Echoview software v4.1 (<http://www.echoview.com>) and involved subtraction in the linear domain of mean backscatter from a 10 ping subset within each transect which displayed no evidence of fish presence. A minimum volume backscatter threshold of 12 dB was set to remove remaining noise and false targets. At a

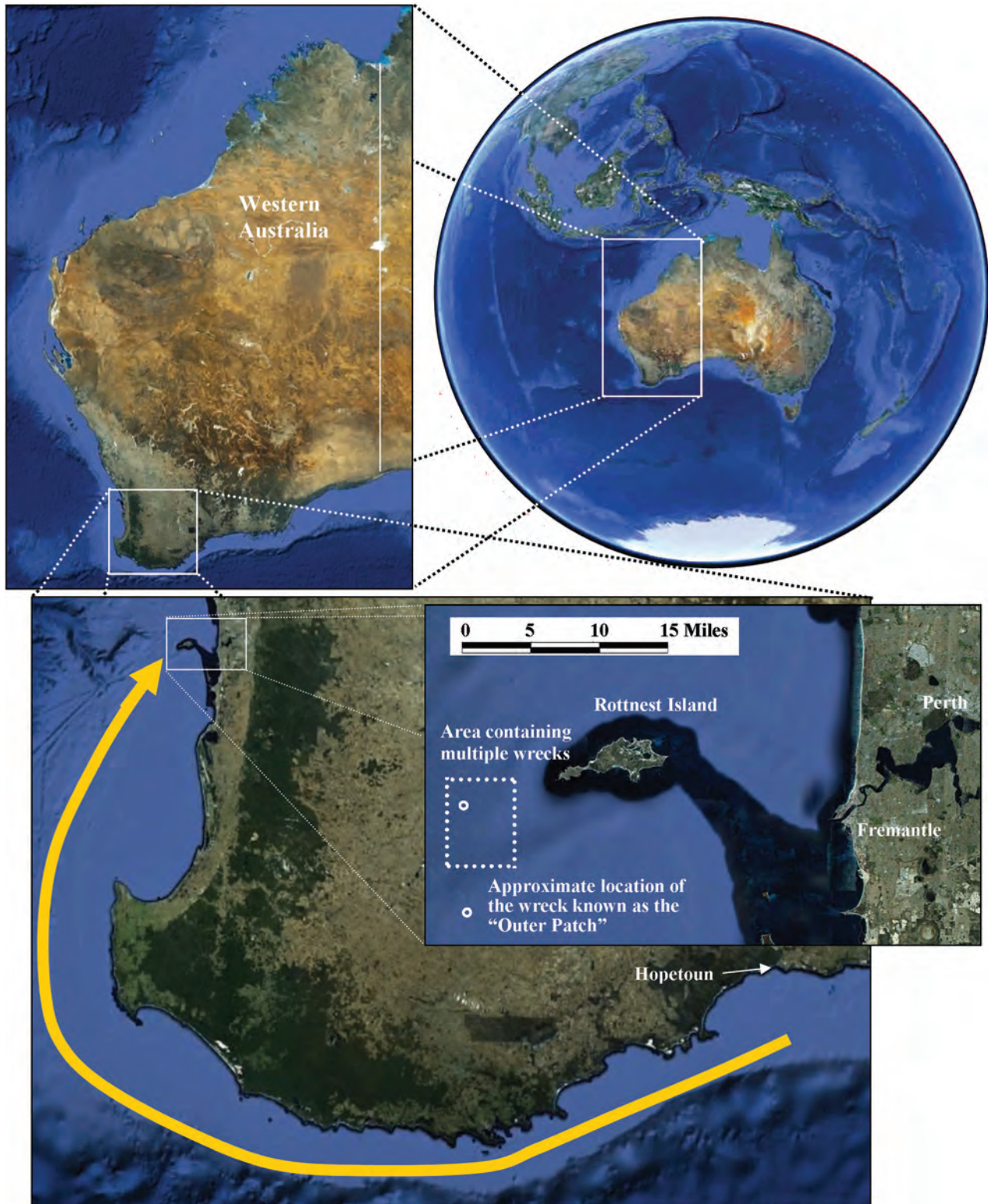


Figure 1. Map of Western Australia with insets magnifying the southwest corner and Rottneest Island. The migration route of *S. hippos* from Hopetoun around to Rottneest Island is depicted by the orange arrow. An area containing a number of wrecks known to attract spawning aggregations of *S. hippos* in the summer is shown by the white dotted rectangle. The white circle denotes the approximate location of the "Outer Patch" wreck. (Image source Google Earth, 06/01/2013).

range of 100 m, where targets were predominantly detected, removed noise was typically in the region of 16 dB. After this noise subtraction, the remaining backscatter was predominantly attributable to seabed and fish; however, not all noise was removed below the seabed and in the outer beams (Figure 2). Visual scrutiny of successive pings was used to determine if remaining samples were noise and, if so, the samples were discarded. Samples were considered to be noise based on the same equivalent sample position in neighbouring pings (i.e. the same beam and range) and their position relative to known noise artefacts (previously identified locations of side lobes and electrical noise within the swathe). The noise displayed in Figure 2 was typical of backscatter acquired in all transects, although in some instances pings of irreconcilable noise (nominally due to vessel slap) were discarded (typically 1 ping per transect). Echoview two-dimensional school detection algorithms were run to identify *S. hippos* acoustic targets within individual pings at height, width, and length dimensions of > 0.02 m (i.e. a size smaller than one sample volume). Pings were then visually scrutinized again, and any remaining samples attributed to noise were manually identified and removed. As the information on each ping was only two-dimensional, for visualization purposes each detected target was then extended through 1 m within Echoview to form an object that represented the fish.

The swimbladder size of *S. hippos* is considerably larger, dorso-ventrally, than each Reson 7125 sample volume size. As a result, the acoustic reflectance from a single *S. hippos* encompasses several samples, both along a single beam and across multiple beams. An acoustic target, representing an individual fish, therefore comprises a cluster of samples (all probably connected) of varying backscatter values, and a cluster of unconnected (occasionally connected when fish swim close together) acoustic targets represent the aggregation of *S. hippos* (Figure 2b, top right). GPS and motion sensor data were imported into Matlab, and swathe target positions were adjusted for roll and heading before being geo-referenced in Cartesian coordinates. Swathe positions and volume backscatter values were exported into Matlab to calculate aggregation volumes using Myriax-developed Matlab programs (B. Buelens, Myriax, pers. comm.). Individual acoustic targets were linked to their three nearest neighbours to form a tetrahedron, and each tetrahedron linked together to form an overall volume which encompassed the acoustic targets and therefore the entire aggregation. A maximum target linking distance was used to exclude or include individual targets from the aggregation, based on how far away each target was from the other fish. Threshold distances between targets were tested at 1 m intervals to observe at what linking distance the targets were separated, and final thresholds were set once 85% of all detected targets were encompassed within the calculated aggregation volume. This linking distance was determined to be 9 m. For coherence, the same linking distance was applied to all transects.

Seabed acoustic backscatter was corrected for angular dependence using Matlab programs developed by the Centre for Marine Science and Technology (CMST). The algorithm works by removing the mean and standard deviation angular trends before restoring local mean levels to acoustic backscatter (Parnum, 2008). The algorithm can be expressed in the following form:

$$BS_{\text{Cor}}(\theta) = \frac{BS(\theta) - \overline{BS}(\theta)}{BS_{\text{std}}(\theta)} + \overline{BS}(30^\circ) \quad (1)$$

where $BS(\theta)$, $BS_{\text{Cor}}(\theta)$, $BS_{\text{std}}(\theta)$, and $\overline{BS}(\theta)$ are the uncorrected, corrected, standard deviation, and mean backscatter for all data at angle θ , respectively. The mean backscatter for all data at 30° is added to provide comparable absolute values derived after corrections (Parnum, 2008). Corrected backscatter was then compared with depth data for seabed classification.

Results

The *S. hippos* aggregation was observed over several transects, and in each case individual targets were detected by the Reson 7125 Seabat, and processed using Echoview MBS school detection modules. Acoustic targets rarely comprised single samples, but clumps of samples containing volume backscatter values above the noise threshold level (see Figure 2). Such targets resembled the nature of acoustic backscatter expected from individual *S. hippos*. These clusters of samples were separated by a distance comparable with the expected distance between individual *S. hippos*, implying that a cluster of samples represented an individual fish (Figure 2). Considerable variation in backscatter was observed across both the aggregation and the clusters of samples that made up an individual fish target (Figure 3). The samples ranged in backscatter by 15 dB, even at the same angle of incidence.

In previous studies, the aggregations of *S. hippos* were thought to remain relatively sedentary over long periods (Parsons et al., 2005). Transects conducted between 10:05:30 and 10:17:45 on 3 February 2007 displayed evidence of the mobility of the aggregation over short periods, as shown in Figure 4. The aggregation was observed to move from close to the eastern side of the wreck to the north end, and then down to the far southeast side over ~ 91 m (substantial mobility by comparison with the opinion of general fishers). In each transect, the aggregation was observed to be at the side of the cruisetrack and not directly beneath (Figure 4, green lines), similar to behaviour observed during transects at other sites during this survey. This is in contrast to previous surveys, where the *S. hippos* have been positioned directly below the survey vessel (Parsons et al., 2006).

Transects were commenced at ~ 3 min intervals (Figure 4). There was a significant change from the 10:11am transect (conducted south to north), where 740 acoustic targets were located north of the wreck (Table 1), and the 10:14 am line, where 2426 acoustic targets were spread along the eastern side of the wreck (Figure 4). In these cases, the change was not only in the number of targets, but also in the plan area and volume of the aggregation (Table 1), though there was no apparent variation in vertical distribution or nearest-neighbour distances between targets in a single ping. Mean acoustic volume per target for the Reson 7125 survey was found to be relatively consistent throughout transects of the site, at 12.7 ± 2.4 m³ per target ($n = 5$), equivalent to $\sim 1.6 \pm 0.1$ body lengths nearest-neighbour distance. This does not, however, consider targets between pings which were not sampled.

Seabed acoustic backscatter produced considerable data from which it was possible to classify the habitat beneath the aggregation. Bathymetric data identified flat sand at 112.5 m depth surrounding a wreck, partially buried, that protruded up to 3 m out of the sand (Figure 5a). To the east of the wreck, a rise in bathymetry (111 m) and to the southwest a longitudinal depression (to ~ 113.5 m) were also observed. Areas of no data were present to the east and west of the wreck (Figure 5, white areas). Elevated levels of backscatter were observed, as expected, in the nadir beams,

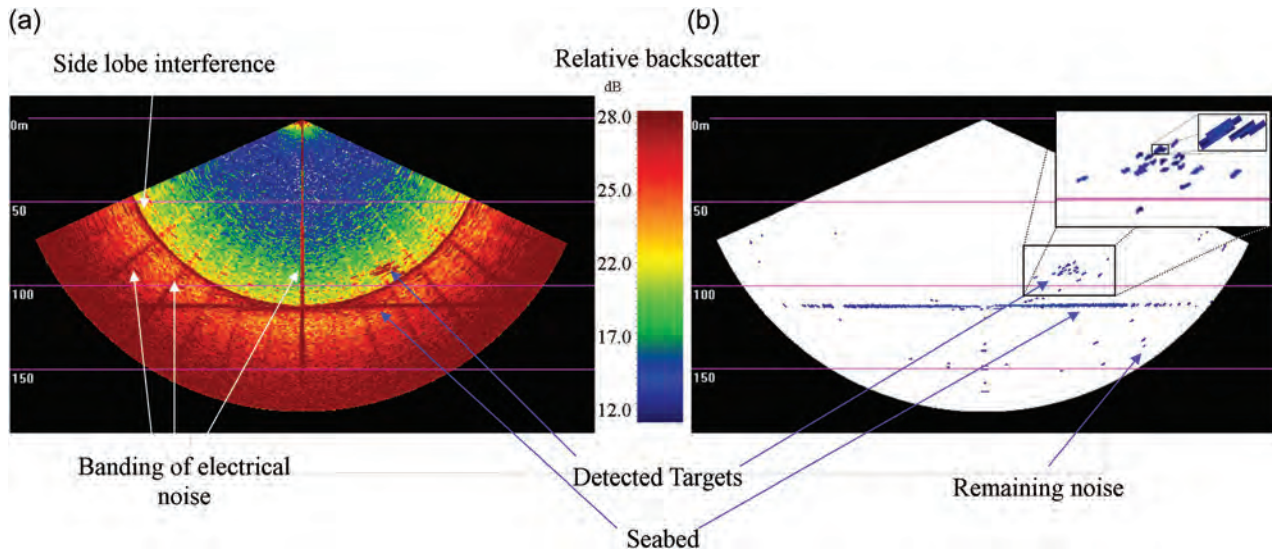


Figure 2. Example RESON 7125 Seabat acoustic swathe of aggregating *S. hippos* displaying an echogram before (a) and after (b) acoustic noise removal. Volume backscatter values were thresholded at 12 and 28 dB, graduated as per the colour bar. Coherent electrical noise, side-lobe noise (“spoking”), together with detected targets and seabed are highlighted. Insets show expansions of detected targets highlighting one target comprising a cluster of several samples (top right).

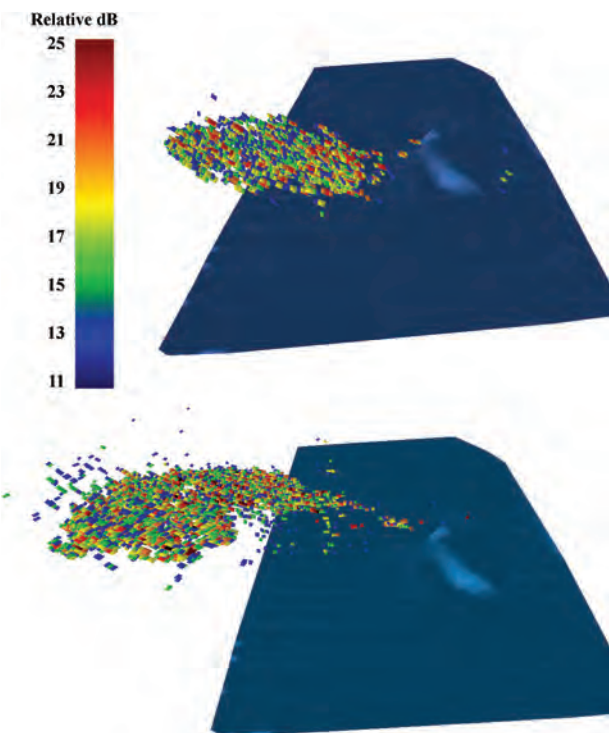


Figure 3. Three-dimensional visualization of a *S. hippos* aggregation at 10:11:44 (a) and 10:14:18 (b). Detected individual samples are coloured as per the colour bar to their respective acoustic backscatter.

coincidentally along the line of the wreck (Figure 5b). The corrected backscatter confirmed the wreck as a rougher surface (i.e. relatively high S_a) than the surrounding area of sand (i.e. relatively low S_a ; Figure 5c). Elevated bathymetry east of the wreck produced the lowest area of backscatter, and the longitudinal depression to the southwest produced relatively high backscatter.

Comprehensive images of the aggregating *S. hippos* and the habitat around which they spawn were produced (Figure 6). This allowed visualization of the entire aggregation as a group of individually detected samples separated by backscatter bins (Figure 6a) and/or encompassing aggregation volumes relative to the wreck (Figure 6b). Aggregation movement during multiple transects was observed in the differing positions of the aggregation volume around the wreck (Figure 6c). It was observed that over the course of the transects, the aggregation appeared to move in a clockwise circle where the centroid of the aggregation moved ~ 91 m, over a 15 min period.

Discussion

The Reson 7125 collected acoustic backscatter from entire aggregations of *S. hippos* in a single 3 min transect, detecting fish in depths of up to 100 m. The data acquisition and processing techniques have produced high-resolution images of entire aggregations and their associated habitat. *Seriola hippos* were imaged as acoustic targets representing individual fish (each comprising a cluster of several samples) and as an aggregation (represented by a group of separated acoustic targets). The combination of interping distance and alongship beam volume meant that the water was sampled every 0.73–1.83 m (excluding along-track pitch and yaw) taken every 1.2 s (the maximum rate available with the Reson 7125 using a 175 m range). This sampling rate significantly reduced the likelihood of not detecting fish positioned between pings, compared with that of a previous survey conducted with a Reson 8125 MBS (Parsons, 2010).

Anecdotal evidence from fishers suggested that *S. hippos* aggregations can be mobile around the wrecks they surround. Single-beam surveys of *S. hippos* suggested movement of the aggregation, although they could not confirm it (Parsons et al., 2005; Parsons, 2010), and a previous MBS survey conducted over the same site did not detect any lateral movement of the aggregation (Parsons, 2010). The five transects described here have shown

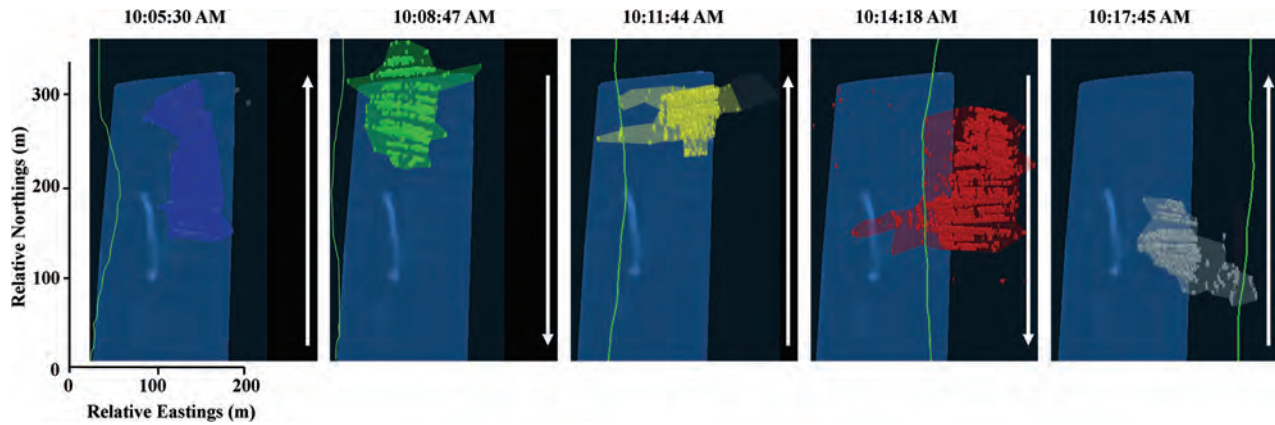


Figure 4. Plan views of five consecutive acoustic transects displaying aggregation movement during a 15 min period, with transect start times noted above. The seabed is shown in blue, and fish regions generated from backscatter are shown in various colours, bounded by the aggregation volume. Cruisetracks are shown by green lines, and vessel direction by the white arrows.

Table 1. Density packing of acoustic targets observed in transects of the *S. hippos* aggregation at the “Outer Patch”.

Transect start time	Aggregation volume at 9 m linking (m^3)	Number of acoustic targets	Acoustic target density packing (m^3 per target)
10:05:30	6159	407	15.1
10:08:47	3482	252	13.8
10:11:44	6425	669	9.6
10:14:18	31 856	2227	14.3
10:17:45	9225	846	10.9

that this speculation of mobility is correct, and that the aggregations do not necessarily remain sedentary.

With each reciprocal transect, the number of detected targets and the aggregation volume changed (exemplified by the 10:11 and 10:14 transects). A lack of change in acoustic target density between transects suggested two possible explanations for this variation. The first is that a large influx and exodus of fish was occurring between transects. Such an explanation is unlikely, given the short space of time between transects, and would most probably be detected on the MBS data. However, the second possibility was that in the 10:14 transect, the aggregation moved away from the vessel in a uniform group along the direction of vessel travel, which led to multiple detections of the same fish. While the critical sustainable swimming speeds of *S. hippos* have not been reported, another *Seriola* species, *S. lalandi*, can reportedly sustain swimming at 2.11 ± 0.9 fork lengths s^{-1} (Yanase *et al.*, 2012). If the same applied to *S. hippos* in the observed aggregation, this would provide a swimming speed estimate of 4.3 ± 1.7 knots. Anecdotal evidence from towed video transects have shown that the *S. hippos* have no trouble keeping up with the vessel and indeed can swim alongside the video camera. If the aggregation swam parallel to, but away from, the vessel, with consistent nearest-neighbour distances, this type of movement could lead to the detected increase in volume (and elongation of the aggregation) and number of targets (due to multiple detections of individual fish) whilst maintaining the overall acoustic packing density. This suggestion was in part corroborated by the lack of vertical migration shown as the transect was conducted. In comparison, in the previous transect (10:11), the aggregation volume was

shortened as it would be if the aggregation stopped or moved towards the vessel. Thus, it has been inferred that while the number of fish within the aggregation remained similar throughout the transects, they collectively moved around laterally, above the wreck.

The extent of the aggregation movement here is in contrast to that exhibited in a previous MBS study conducted at the beginning of the previous spawning period in October, where the centroid of the aggregation remained relatively sedentary (Parsons, 2010). In that study, a small increase in packing density was observed after a period of fishing; however, no significant lateral movement by the aggregation was observed (Parsons, 2010). Axelsen *et al.* (2000) observed changes in behaviour and aggregation structure in herring (*Clupea harengus*) at different times during the spawning period. It is feasible that the *S. hippos* aggregations are more mobile and/or likely to react to vessel presence towards the end of the spawning season than the beginning, which would contribute to the differences in aggregation movement observed in the two MBS surveys at the Outer Patch.

Movement of fish schools due to vessel avoidance is complex and is being increasingly studied using MBS systems (Soria *et al.*, 1996; Gerlotto *et al.*, 2004; Weber *et al.*, 2007). Balchen (1984) suggested that vessel avoidance is a result of sound and visual stimuli, and natural behaviour. While not all fish species exhibit vessel avoidance at all times (Ona and Torezen, 1988; Ona and Godø, 1990), many fish species exhibit avoidance behaviour prior to a visual stimulus (Olsen *et al.*, 1983b; Diner and Masse, 1987; Soria *et al.*, 1996; Gerlotto *et al.*, 2004), others avoid the vessel once within visual distance and/or when the vessel passes above (Soria *et al.*, 1996), and some species only avoid it if under the direct path of the vessel (Diner and Masse, 1987). Vessel avoidance prior to visual stimuli will be partially dependent on the hearing frequency and sensitivity of the species. Variation in vessel avoidance within a species has been proposed to be a function of fish depth (Misund, 1997), fish range (Olsen *et al.*, 1983b; Diner and Massé, 1987; Fréon *et al.*, 1992; Soria *et al.*, 1996), vessel speed (Olsen *et al.*, 1983b), vessel size (Olsen *et al.*, 1983a), noise propagation (Engås *et al.*, 1995; Gerlotto *et al.*, 2004), and ontogenetic stage (Neproschin, 1979; Misund, 1993). It is therefore likely that vessel avoidance will vary significantly over time, as environmental, acoustic, and behavioural conditions

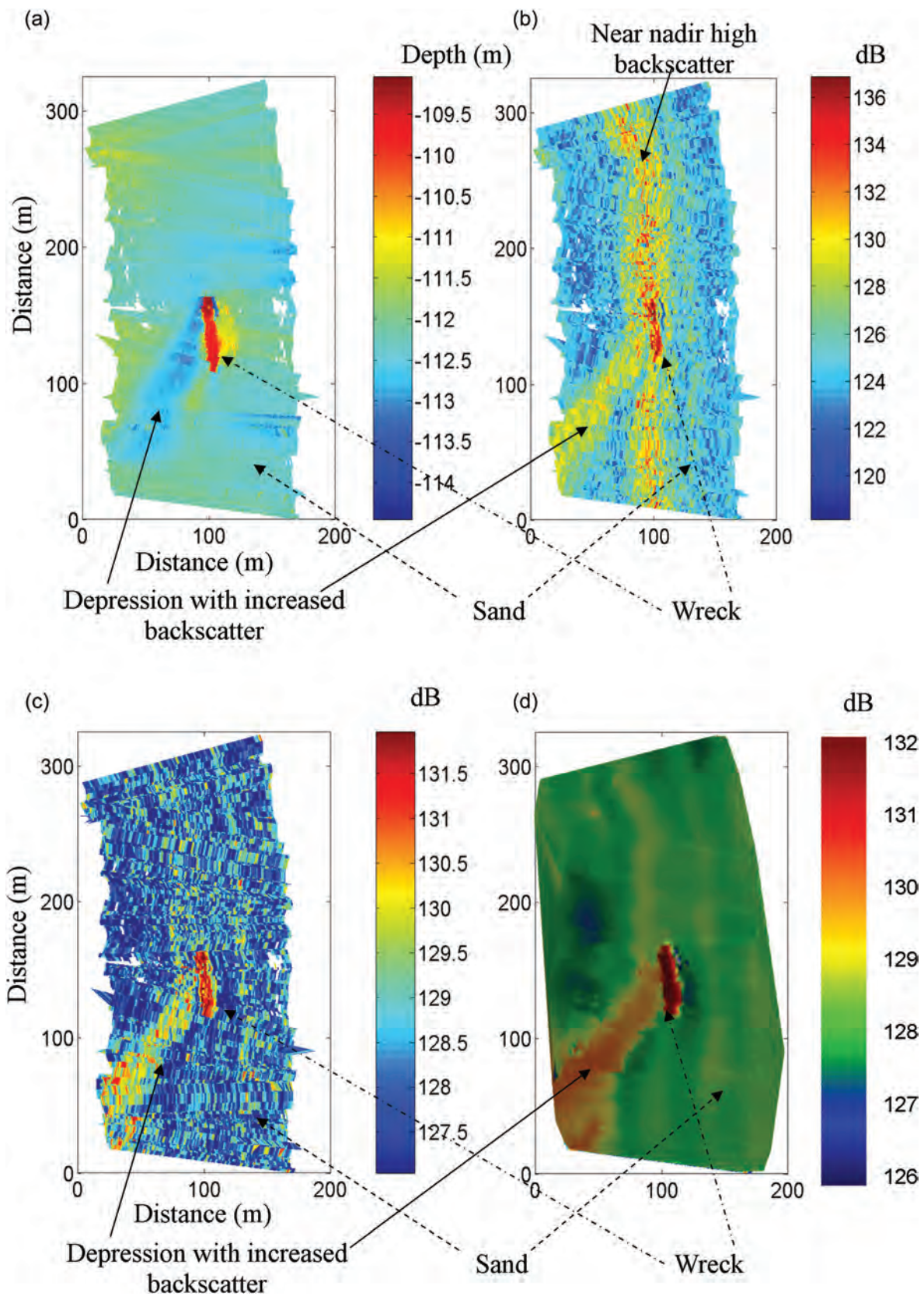


Figure 5. Bathymetry (a), uncorrected backscatter (b), corrected backscatter (c), and smoothed backscatter (d) acquired from a single acoustic transect of the Outer Patch site. Axes display relative distance in metres, while depth and relative backscatter are shown as per the respective colour bars.

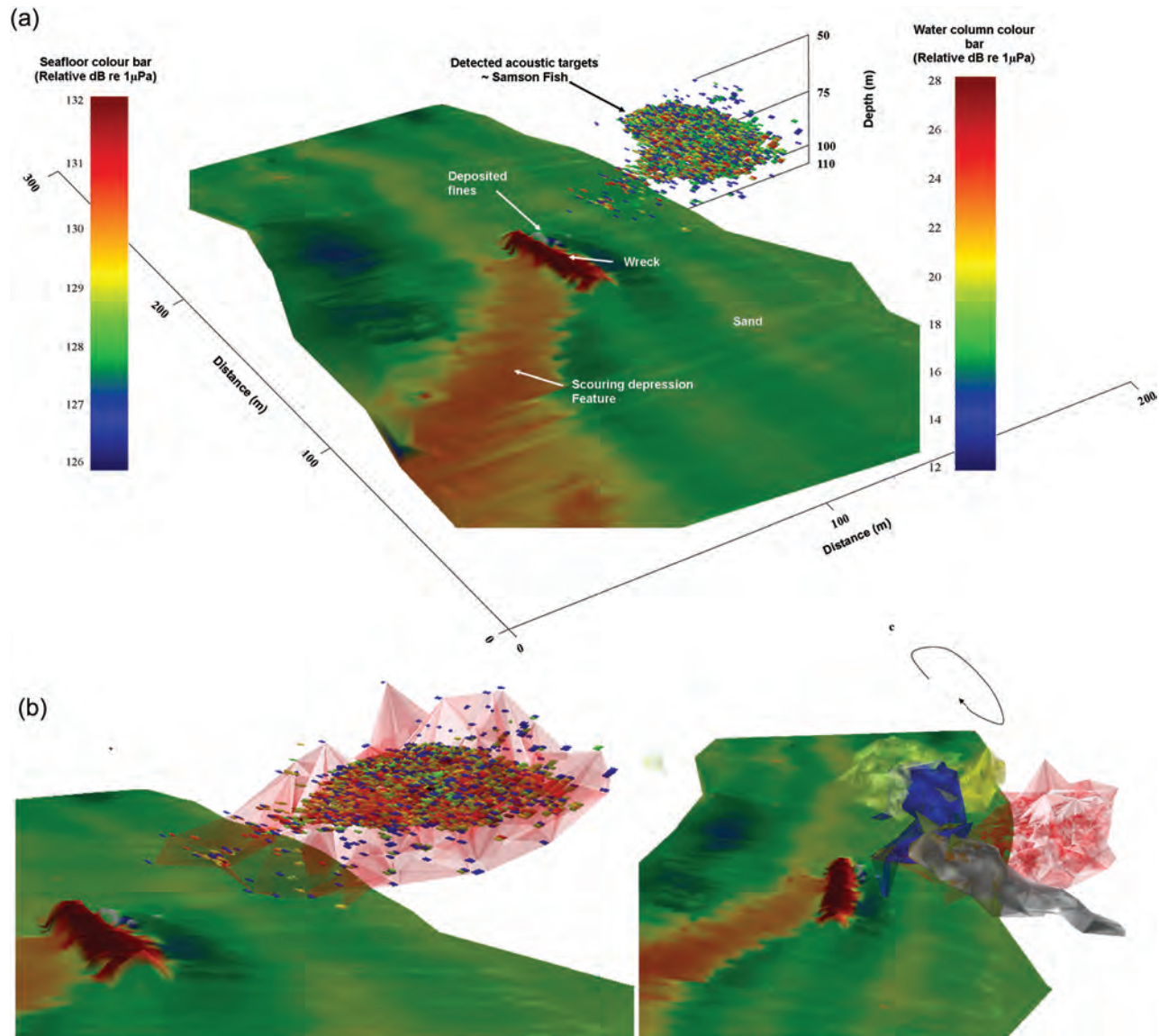


Figure 6. Three-dimensional visualization of the seabed and the *S. hippos* aggregation at the Outer Patch with colouring of surface and volume backscatter as per the respective colour bars (a). Acoustic targets separated by $< 12\text{ m}$ enclosed within an aggregation volume (red) where the opacity of each part of the aggregation volume “bubble” represents target density within the aggregation (b). Aggregation movement during five transects, each separated by $\sim 3\text{ min}$, running order: blue, green, yellow, red, and finally grey (motion highlighted by grey arrow) (c).

change. These causes of avoidance could contribute to the difference in *S. hippos* packing density behaviour between transects conducted in October, at the beginning of the spawning season (Parsons *et al.*, 2006), and those at the end of the season reported here.

Vessel avoidance could explain the elongation of the aggregation such as that of the 10:14 transect, but does not explain the small volume of the aggregation in the 10:11 transect. The *S. hippos* aggregation demonstrated the tendency to alter movement direction between transects. It is possible that an attraction to a habitat-related structure from which the fish maintain a maximum distance could result in apparent variations in movement with differing vessel position and direction. That is, the aggregation may avoid the survey vessel up to a maximum distance from the wreck before stopping. Submerged structures alter the

local current field, and there is evidence that some species of pelagic fish position themselves up-current of these structures (Lindquist and Pietrafesa, 1989; Capello *et al.*, 2012), with their position and range from the structure driven in part by the strength of the current (Capello *et al.*, 2012).

It is important to observe not only the fish school, but also the habitat and environment within which they spawn. The Reson 7125 seabed backscatter data produce habitat images comprising not only the expected differences between wreck and sand, but identifying features not previously described, namely the build up of low backscatter sediment to the east of the wreck and depression of high backscatter to the southwest. The most likely explanation for this phenomena is the sediment transfer of fine particles due to a current from the northeast, i.e. scouring. The two features

of accretion of fine sand on the “updrift”, eastern side (exhibiting relatively lower backscatter than the surrounding sandy seafloor) and the area with fine sand removed towards the southwest, of higher relative backscatter, are similar to that of other sites of wrecks where scouring occurred in areas of low current (DeAlteris, 1975; Caston, 1979; Quinn *et al.*, 1997). This is compared with sites in high current where a scour hollow would also be expected on the up-current side of the wreck. During the Western Australian summer, two currents dominate the broad-scale movement of water; the southbound “Leeuwin Current” which runs all year round, and underneath it the northbound “Capes Current”, which is strongest during the summer. Interaction between the Capes and Leeuwin currents at the location of the wreck graveyard suggest the likelihood of a weak northeasterly current at the seabed during the summer period (Rennie, 2007). Transects at this site therefore suggest that the aggregation prefers to position itself up-current of the protruding wreck. However, aggregation positions recorded here earlier in the season, and at other sites, were directly above the wreck (Parsons, 2010). It is possible that this behaviour is due to a variation in the current field; however, this is speculation and requires further investigation.

Concluding remarks

This study has shown that MBS systems can detect movement patterns of pelagic schools of fish and at the same time map the habitat they surround. While there is not the evidence to determine the reasons behind the aggregation position relative to the habitat, or the behaviour of the fish, it has highlighted that the two can be detected. There are a number of biological and environmental drivers and anthropogenic activities that contribute to the dynamic behaviour of fish schools/aggregations at the time of the survey. Many of these are already regularly investigated, such as fish depth, fish range, vessel speed, noise propagation, species hearing thresholds, visual field, ontogenetic stage, and fishing activity, while others, such as the strength of affiliation with spawning habitat and the effects of the current field, have been studied to a lesser extent. These factors are interdependent, and for aggregations may well vary with point of time in the spawning period. Modelling school/aggregation responses to all of these drivers is important to better understand the MBS data derived from surveys of pelagic and demersal fish and so fish behaviour.

Acknowledgements

The authors would like to acknowledge: Reson for the supply of equipment and technical expertise, particularly Chris Malzone for arranging the equipment; the Australian Government via the Fisheries Research and Development Corporation (FRDC) for funding; Western Australia Department of Fisheries for the availability and use of the RV *Naturaliste*; Myriax for Echoview software and technical support with which water column data were processed (in particular Matt Wilson, Bart Buelens, and Myounghee Kang); and the Centre for Marine Science and Technology for their expertise in acoustic processing techniques. A PhD top-up was gratefully received from the Western Australian Marine Science Institute (WAMSI).

References

Andersen, L. N., Berg, S., Gammelsaeter, O.B., and Lunde, E. B. 2006. New scientific multibeam systems for fishery research applications.

- In* Eighth European Conference on Underwater Acoustics. Ed. by S. M. Jesus, and O. C. Rodriguez. Carvoeiro, Portugal.
- Axelsen, B. E., Nøttestad, L., Fernö, A., Johannessen, A., and Misund, O. A. 2000. ‘Await’ in the pelagic: dynamic trade-off between reproduction and survival within a herring school splitting vertically during spawning, *Marine Ecology Progress Series*, 205: 259–269.
- Balchen, J. G. 1984. Recent progress in the control of fish behaviour. *Journal of Modelling Identification and Control*, 52: 113–121.
- Brown, C. J., and Blondel, P. 2009. Developments in the application of multibeam sonar backscatter for seafloor habitat mapping. *Applied Acoustics*, 70 (10): 57–84.
- Brown, C. J., Smith, S. J., Lawton, P., and Anderson, J. T. 2011. Benthic habitat mapping: a review of progress towards improved understanding of the spatial ecology of the seafloor using acoustic techniques. *Estuarine, Coastal and Shelf Science*, 92: 502–520.
- Buelens, B., Wilson, M., and Horne, J. K. 2007. Multi-beam water column data analysis for fisheries research: a worked example in Echoview. *In* 2nd International Conference on Underwater Acoustic Measurements: Results and Technologies, pp. 669–677. Heraklion, Crete.
- Capello, M., Soria, M., Potin, G., Cotel, P., and Dagorn, L. 2012. Role of Current and Daylight Variations on Small-pelagic Fish Aggregations Around a Coastal FAD from Accurate Acoustic Tracking. Cornell University Library, 16 pp., arXiv:1202.4278
- Caston, G. F. 1979. Wreck marks: indicators of net send transport. *Marine Geology*, 33: 193–204.
- Castro, J. J., Santiago, J. A., and Santana-Ortega, A. T. 2002. A general theory on fish aggregation to floating objects: an alternative to the meeting point hypothesis. *Reviews in Fish Biology and Fisheries*, 11: 255–277.
- Chu, D., Foote, K. G., and Hufnagle, J. L. C. 2002. Measurement of multi-beam sonar directivity patterns. *In* MTS/IEEE Oceans 2002, pp. 1411–1414.
- de Alteris, J. T., Roney, J. R., Stahl, L. E., and Carr, C. 1975. Sediment transport study offshore New Jersey. *Civil Engineering in the Oceans III*, 1: 225–244.
- Diner, N., and Masse, J. 1987. Fish School Behaviour During Echo Survey Observed by Acoustic Devices. ICES Document CM 1987/B30: 28 pp.
- Domeier, M. L., and Colin, P. L. 1997. Tropical reef fish spawning aggregations: defined and reviewed. *Bulletin of Marine Science*, 60: 698–726.
- Engås, A. E., Misund, O. A., Soldal, A. V., Horvei, B., and Solstad, A. 1995. Reactions of penned herring to playback of original, frequency filtered and time-smoothed vessel sound. *Fisheries Research*, 22: 243–254.
- Foote, K. G., Chu, D., Hammar, K. C., Baldwin, L. A., Mayer, L. C., Hufnagle, J., and Jech, M. J. 2005. Protocols for calibrating multi-beam sonar. *Journal of the Acoustical Society of America*, 114: 2013–2027.
- Freon, P., Gerlotto, F., and Misund, O. A. 1993. Consequences of fish behaviour for stock assessment. *ICES Journal of Marine Science*, 196: 181–191.
- Gerlotto, F., Castillo, J., Saavedra, A., Barbieri, M. A., Espejo, M., and Cotel, P. 2004. Three dimensional structure and avoidance behaviour of anchovy and common sardine schools in central southern Chile. *ICES Journal of Marine Science*, 61: 1120–1126.
- Holmin, A. J., Tjøstheim, D., and Korneliussen, R. 2009. Identification and characterisation of fish schools using the Simrad MS70 3-D multi-beam sonar. *In* International Conference on Underwater Acoustic Measurements: Technologies and Results, 28 June–1 July. Heraklion, Crete.
- Karnauskas, M., Cherubin, L. M., and Paris, C. B. 2011. Adaptive significance of the formation of multi-species fish spawning aggregations near submerged capes. *PLoS One*, 6: e22067.
- Korneliussen, R. J., Heggelund, Y., Eliassen, I. K., Øye, O. K., Knutsen, T., and Dalen, J. 2009. Combining multibeam-sonar and

- multifrequency echosounder data: examples of the analysis and imaging of large euphausiid schools. *ICES Journal of Marine Science*, 66: 991–997.
- Lindquist, D. G., and Pietrafesa, L. J. 1989. Current vortices and fish aggregations: the current field and associated fishes around a tugboat wreck in Onslow Bay, North Carolina. *Bulletin of Marine Science*, 44, 533–544.
- Malzone, C., Lockhart, D., Meurling, T., and Baldwin, M. 2008. The progression and impact of the latest generation of multi-beam acoustics upon multidisciplinary hydrographic-based applications. *International Journal of the Society of Underwater Technology*, 27: 151–160.
- Mayer, L., Li, Y., and Melvin, G. 2002. 3D visualization for pelagic fisheries research and assessment. *ICES Journal of Marine Science*, 59: 216–225.
- Misund, O. A. 1993. Dynamics of moving masses: variability in packing density, shape, and size among herring, sprat, and saithe schools. *ICES Journal of Marine Science*, 50: 145–160.
- Misund, O. A. 1997. Underwater acoustic in marine fisheries and fisheries research. *Reviews in Fish Biology and Fisheries*, 7: 1–34.
- Neproshin, A. Y. 1979. Behaviour of the pacific mackerel, *Pneumatophorus japonicus*, when affected by vessel noise. *Journal of Ichthyology*, 18: 695–699.
- Olsen, K., Angell, J., Pettersen, F., and Løvik, A. 1983a. Observed fish reaction to a surveying vessel with special reference to herring, cod, capelin and polar cod. *FAO Fisheries Report* 300. pp. 131–138.
- Olsen, K., Angell, J., and Løvik, A. 1983b. Quantitative estimations of the influence of fish behaviour on acoustically determined fish abundance. *FAO Fisheries Report* 300. pp. 140–145.
- Ona, E., Dalen, J., Knudsen, H. P., and Patel, R. 2006. First data from sea trials with the new MS70 multibeam sonar. *Journal of the Acoustical Society of America*, 120: 3018.
- Ona, E., and Godø, O. R. 1990. Fish behaviour and trawl geometry observed with scanning net-sonde sonar. *Rapports et Procès-Verbaux des Reunions du Conseil International pour l'Exploration de la Mer*, 189: 159–166.
- Ona, E., and Toresen, R. 1988. Reactions of Herring to Trawling Noise. *ICES Document CM 1988/B*: 36.
- Parnum, I. M. 2008. Benthic habitat mapping using multibeam sonar systems. PhD thesis, Curtin University of Technology. 204 pp.
- Parnum, I. M., and Gavrilov, A. N. 2011a. High-frequency multibeam echo-sounder measurements of sea floor backscatter in shallow water: Part 1. Data acquisition and processing. *International Journal of the Society for Underwater Technology*, 30: 3–12.
- Parnum, I. M., and Gavrilov, A. N. 2011b. High-frequency multibeam echo-sounder measurements of sea floor backscatter in shallow water: Part 2. Mosaic production, analysis and classification. *International Journal of the Society for Underwater Technology*, 30: 13–26.
- Parsons, M. J. G. 2010. Active acoustic techniques for monitoring fish aggregations. In *An investigation into active and passive acoustic techniques to study aggregating fish species*. PhD thesis, Curtin University, pp. 44–131.
- Parsons, M. J. G., McCauley, R. D., and Mackie, M. C. 2005. Preliminary analysis of singlebeam acoustic data of fish spawning aggregations along the Western Australian coastline. *Acoustics, Conference Proceedings of the Australian Acoustical Society, Busselton*. pp. 405–409.
- Parsons, M. J. G., McCauley, R. D., and Mackie, M. C. 2006. Evaluation of acoustic backscatter data collected from Samson fish (*Seriola hippos*) spawning aggregations in Western Australia. Eighth European Conference on Underwater Acoustics, Caroeiro, Portugal. pp. 347–352.
- Patel, R., and Ona, E. 2009. Measuring herring densities with one real and several phantom research vessels. *ICES Journal of Marine Science*, 66: 1264–1269.
- Pikitch, E. K., Santora, C., Babcock, E. A., Bakun, A., Bonfil, R., Conover, D. O., Dayton, P., et al. 2004. Ecosystem-based fishery management. *Science*, 305: 346–347.
- Quinn, R., Bull, J. M., and Dix, J. K. 1997. The Mary Rose site—geophysical evidence for palaeo-scour marks. *International Journal of Nautical Archaeology*, 26: 3–16.
- Rennie, S. J. 2007. Oceanographic processes in the Perth Canyon and their impact on productivity. PhD thesis, Curtin University of Technology. pp. 82–109.
- Reson Incorporated. 2007. Seabat 7125 Operator Manual, version 5'. Reson Inc., Goleta, CA.
- Rowland, A. J. 2009. The biology of Samson Fish *Seriola hippos* with emphasis on the sportfishery in Western Australia. PhD thesis, Murdoch University, 215 pp.
- Soria, M., Freon, P., and Gerlotto, F. 1996. Analysis of vessel influence on spatial behaviour of fish schools using a multi-beam sonar and consequences for biomass estimates by echo-sounder. *ICES Journal of Marine Science*, 53: 453–458.
- Stienessen, S. C., Weber, T. C., and Wilson, C. D. 2009. Use of a multi-beam sonar to characterize fish aggregations in the northern Pacific. *Journal of the Acoustical Society of America* 126: 2233.
- Trenkel, V., Mazauric, V., and Berger, L. 2006. First results with the new scientific multibeam echo-sounder ME70. *Journal of the Acoustical Society of America*, 120: 3017.
- Trenkel, V. M., Mazauric, V., and Berger, L. 2008. The new fisheries multibeam echosounder ME70: description and expected contribution to fisheries research. *ICES Journal of Marine Science*, 65: 645–655.
- Trevorrow, M. V. 2005. Volumetric multi-beam sonar measurements of fish, zooplankton and turbulence. In *International Conference on Underwater Acoustic Technologies: Measurements and Results*, 28 June–1 July. Heraklion, Crete.
- Weber, T. C., Pena, H., and Jech, M. J. 2007. Combining single frequency multi-beam with multi-frequency single-beam sonars: an example with atlantic herring. In *2nd International Conference on Underwater Acoustic Measurements: Technologies and Results*. Heraklion, Crete, pp. 661–668.
- Wilson, M., Higginbottom, I. R., and Buelens, B. 2005. Four-dimensional visualisation and analysis of water column data from multi-beam echosounders and scanning sonars using Sonardata Echoview for fisheries applications. In *International Conference on Underwater Acoustic Measurements: Technologies and Results*, 28 June–1 July. Heraklion, Crete.
- Yanase, K., Neill, A., Herbert, N. A., and Montgomery, J. C. 2012. Disrupted flow sensing impairs hydrodynamic performance and increases the metabolic cost of swimming in the yellowtail kingfish, *Seriola lalandi*. *Journal of Experimental Biology*, 215: 3944–3954.

Handling editor: David Demer